

Differential cross sections for double excitation of the autoionizing states of helium by 100–150 keV proton impact

A L Godunov¹, P B Ivanov², V A Schipakov² and M Schulz³

¹ Department of Physics, Tulane University, New Orleans, LA 70118-5698, USA

² Troitsk Institute for Innovation and Fusion Research, Troitsk, 142092, Russia

³ Department of Physics, University of Missouri-Rolla, Rolla, MO 65409, USA

Received 5 December 2001

Published 24 May 2002

Online at stacks.iop.org/JPhysB/35/2477

Abstract

Autoionizing $(2s^2) ^1S$, $(2p^2) ^1D$ and $(2s2p) ^1P$ resonances in projectile energy loss spectra are studied theoretically for protons scattered on atomic helium. The differential resonance yield, as a function of the scattering angle, is the quantity of primary attention. The effects of the Coulomb interaction in the final state and the projectile–core interaction on the differential resonance yield are studied. Comparison with the experimental data of Schulz *et al* (1995) (Schulz M, Htwe W T, Gauss A D, Peacher J L and Vajnai T 1995 *Phys. Rev. A* **51** 2140–50) is presented. Comparison is also made with calculations for differential cross sections of double excitation.

1. Introduction

Most doubly excited atomic states lie energetically above the ionization threshold, and as a result are strongly coupled to the adjacent electron continuum. Since the probability of the non-radiative (Auger) decay for the low-lying autoionizing states (AIS) of light atoms is several orders greater than the probability of radiative decay (Stolterfoht 1987) the result of the excitation of the AIS can be seen as resonances in the ionization cross sections. Therefore, this peculiarity poses two principal problems for the study of double electron excitation of atoms in collision with charged particles:

- (i) the theoretical definition of the cross section for excitation of AIS taking into account the strong interaction with the continuum, and
- (ii) procedures for experimental measurements of such characteristics.

Considerable progress in this direction has only been very recently achieved (Godunov *et al* 1997a, 2000, Moretto-Capelle *et al* 1997).

Autoionizing resonances in ion–atom collisions have attracted much attention, being extensively studied in various aspects (Stolterfoht 1987, Schulz 1995). The experimental

base of such research has been considerably enhanced over the last few years. Since there are three particles in the final state, various types of experiments can be staged, depending on which particles are to be detected. In a complete experiment, the quantum states of two particles can be measured simultaneously, the energy and momentum of the third particle being determined from the conservation laws. *The multiple differential cross sections* obtained in such experiments contain all the possible information on the mechanisms of AIS excitation and dynamics of AIS decay, interference of direct and resonant ionization as well as the influence of the Coulomb interaction of the three charged particles in the final state (CIFS) on the ionization process. Coincidence experiments for ion-atom collisions are technically difficult to perform, and it is only recently that results from complete experiments for direct ionization by ion impact have been published (Ullrich *et al* 1994), which are considered a very promising direction of research. However, currently the resolution in such experiments is not sufficient to identify resonances in the electron spectra.

Much interesting information can also be discovered in measurements of *doubly differential cross sections* (DDCS), when the final state of only one particle, specified by its energy and solid angle, is detected. There are two types of such experiments, studying autoionization resonances in either the spectra of ejected electrons (Stolterfoht 1987, Rudd *et al* 1992) or projectile energy loss spectra (Htwe *et al* 1994, Schulz *et al* 1995). The latter technique may be especially interesting since it studies the AIS excitation differential in projectile scattering angle, which cannot be determined in electron spectroscopy experiments. However, there are the same complicating circumstances for both methods: interference of direct and resonant ionization may result in a complex resonance profile. As a result the excitation cross section is no longer directly proportional to the measured intensity of the resonance. Furthermore, this interference disguises the natural (autoionization) width leading to resonance shape peculiarities. Moreover, at intermediate collision energies and small ejection angles, CIFS significantly distorts the shape of autoionization resonances, especially in the ejected electron spectra (Arcuni and Schneider 1987, Moretto-Capelle *et al* 1996). To extract information on mechanisms of AIS excitation from the distorted resonance profiles, they have to be fitted to a parametric formula accounting for all the relevant effects. When such a parametrization is either impossible or inefficient, one can use indirect methods to evaluate excitation cross sections, such as determining differential resonance yields or (Schulz *et al* 1995) investigating charge and charge-sign dependencies (Pedersen and Hvelplund 1989).

Electron spectroscopy of autoionization resonances has the important virtue of the high-energy resolution achieved (Bordenave-Montesquieu *et al* 1995, Moretto-Capelle *et al* 1996) and the availability of a number of parametrizations for different kinematic regions (Fano 1961, Shore 1967, Godunov *et al* 2000). The effects of CIFS and the interference of direct and resonant ionization are essentially dependent on the direction of the ejected electron, and, fitting experimental DDCS to a parametric formula adequately incorporating both factors (Godunov *et al* 1997a), one can extract the excitation cross sections of the lowest lying AIS of helium and their magnetic sublevel population (Moretto-Capelle *et al* 1997, Godunov *et al* 2000). This method is only applicable under conditions where the CIFS is strong and it demands high energy resolution in the experiment. Thus, electron spectroscopy studies have revealed the basic mechanisms of AIS excitation, such as correlated excitation, two-step excitation and the inverse Auger process (transition to a quasi-discrete level via the embedding continuum) and the contributions of specific mechanisms to the total cross section have been estimated (Godunov *et al* 2000).

Projectile energy loss spectra contain information on differential excitation cross sections that could provide evidence for an interplay between different mechanisms of AIS excitation. The resolution in energy loss experiments is still poorer by an order of magnitude (Schulz 1995,

Schulz *et al* 1995). Moreover, there is no adequate and efficient parametrization of this kind of DDCS for strong CIFS. However, this technique allows one to determine differential (in projectile solid angle) yields of autoionization resonances and relate them to AIS excitation cross sections.

Certain progress has been made in studying both differential and doubly differential cross sections of direct ionization (Kamber *et al* 1988a, Schulz *et al* 1996). In particular, the important role of the projectile–core interaction has been revealed in proton impact ionization of atoms, at scattering angles greater than 0.55 mrad (Kamber *et al* 1988b, Schulz *et al* 1996, Godunov *et al* 1998, Rodriguez *et al* 1998). This aspect of heavy-particle collisions with atoms is very difficult to reveal in electron spectra, where small scattering angles contribute most to the averaged cross sections. Energy loss spectroscopy has been further developed to observe, for the first time, autoionization resonances in the spectra of 50–150 keV protons scattered on helium (Schulz *et al* 1995). This experiment incited theoretical interest in doubly differential ionization cross sections, in terms of energy and scattering angle, and was promptly followed by the first close coupling calculations (Martín and Salin 1995), which, however, did not account for CIFS, which is expected to be important in this kinematic region.

The purpose of this work is to theoretically analyse projectile energy loss spectra in the region of autoionization resonances in comparison with the available experimental data (Schulz *et al* 1995). In section 2, the expressions for doubly differential ionization cross sections and differential resonance yields are derived on the basis of a theory of resonant ionization accounting for CIFS (Godunov *et al* 1989), which has succeeded in describing autoionization resonances in the spectra of ejected electrons at intermediate projectile energies (Godunov *et al* 1997a). The results of the calculations for the lowest lying AIS of helium excited by 100–150 keV protons are presented in section 3. The conclusions are summarized in section 4. Atomic units are used throughout this paper, unless otherwise stated.

2. Theory

2.1. Energy loss spectrum

Projectile energy loss spectra are described by *doubly differential* cross sections of scattering projectiles with energy E_f into the solid angle Ω_f . Accounting for both the spectrum of discrete one-electron excitation and a continuous spectrum of states populated either by direct ionization or as a result of the decay of AIS, the projectile scattering DDCS can be expressed as

$$\frac{d^2\sigma}{dE_f d\Omega_f} = (2\pi)^4 m_p^2 \frac{K_f}{K_i} \sum_v \frac{d\sigma_v}{d\Omega_f} \delta(E_i - E_f - E_v) + (2\pi)^4 m_p^2 \frac{K_f k_e}{K_i} \int |t_{fi}(E_i, \Omega_f, \mathbf{k}_e)|^2 d\Omega_e. \quad (1)$$

Here, $d\sigma_v/d\Omega_f$ is the differential cross section of one-electron excitation of the discrete-spectrum level ν of the target with energy E_ν , the second term describes target ionization with the amplitude t_{fi} , \mathbf{K}_i and \mathbf{K}_f are the momenta of the incoming and outgoing projectile, Ω_e is the solid angle of an ejected electron with momentum \mathbf{k}_e and m_p is the mass of the projectile. The discrete component of the spectrum ($E_i - E_f < I$), describing one-electron excitation, has been studied in considerable detail previously (Kvale *et al* 1985). In this work, we shall only consider the continuum component of the spectrum in the vicinity of autoionization resonances.

Our consideration is based on the theory of atomic ionization by charged particle impact (Godunov *et al* 1989, 1997a, 2000). In this paper only key formulae are presented that will be used in the discussion that follows. For intermediate and high collision energies the total

amplitude of target ionization in the region of autoionizing resonances accounting for CIFS in both the direct and resonance channels can be written as

$$t_{\text{fi}}(E_i, \Omega_f, \mathbf{k}_e) = t_{\text{dir}}(E_i, \Omega_f, \mathbf{k}_e) + \sum_{\mu} K_{\text{res},\mu}(E_i, \Omega_f, \mathbf{k}_e) \frac{t_{\text{dec},\mu}^0(\mathbf{k}_e) t_{\text{exc},\mu}(E_i, \Omega_f)}{\varepsilon_{\mu} + i}, \quad (2)$$

where t_{dir} is the amplitude of direct ionization, $t_{\text{exc},\mu}$ is the amplitude of AIS excitation, $t_{\text{dec},\mu}^0$ is the amplitude of AIS decay in the isolated atom, $\mu = \{\gamma_{\mu} LM\}$ is the set of quantum numbers for the AIS and $\varepsilon_{\mu} = 2(E_e - E_{\mu})/\Gamma_{\mu}$ is the relative deviation of the energy E_e associated with the target electrons from the position E_{μ} of the resonance with the width Γ_{μ} . The kinematic factor $K_{\text{res},\mu}(E_i, \Omega_f, \mathbf{k}_e)$, accounts for the influence of the Coulomb interaction in the final state on the AIS decay. The explicit expression for this factor is given elsewhere (Godunov *et al* 1989, 1997a). In the general case, it implies a complex dependence on the projectile energy E_i , electron emission energy E_e (i.e. the relative energy ε_{μ}) and electron ejection angle θ_e , but a relatively weak dependence on the scattering angle in the case of ion–atom collisions. When the interaction in the final state is not very strong, one can use a compact expression for $K_{\text{res},\mu}$ in the eikonal approximation (Godunov *et al* 1997a):

$$K_{\text{res},\mu}(E_i, \Omega_f, \mathbf{k}_e) = f_c^{(+)}(\xi)(\varepsilon_{\mu} + i)^{-i\xi} \exp(i\psi_{\mu}), \quad (3)$$

with $f_c^{(+)}(\xi) = \exp(-\pi\xi/2)\Gamma(1 + i\xi)$ being the norm of the Coulomb wavefunction, and $\xi = \nu_{12} + \nu_{13}$, $\psi_{\mu} = \nu_{12} \ln(2(k_{12}v_f + k_{12}v_f)/\Gamma_{\mu}) + \nu_{13} \ln(4k_{13}v_f/\Gamma_{\mu})$ with $\nu_{ij} = Z_i Z_j/v_{ij}$. Here, indexes 1, 2 and 3 refer to the scattered projectile, ejected electron and residual ion, respectively, $k_{ij} = m_{ij}v_{ij}$ is the momentum of the relative motion of two particles with reduced mass m_{ij} , Z_i is the charge of the i th particle and v_f is the velocity of the scattered particle relative to the target. The influence of the CIFS also results in modification to the direct ionization amplitude t_{dir} . In a particular case it can be reduced to a kinematic factor K_{dir} modifying the first born amplitude (see section 2.3).

Substituting the expression for the total ionization amplitudes (2) in the definition (1) and neglecting interferences between overlapping resonances, we obtain the DDCS of projectile scattering in the region $E_i - E_f > I$ as

$$\frac{d^2\sigma}{dE_f d\Omega_f} = \left(\frac{d^2\sigma}{dE_f d\Omega_f} \right)_{\text{dir}} + \sum_{\mu} \frac{A_{\text{int},\mu}(\Omega_f, \varepsilon_{\mu}) \varepsilon_{\mu} + B_{\text{int},\mu}(\Omega_f, \varepsilon_{\mu}) + B_{\text{exc},\mu}(\Omega_f, \varepsilon_{\mu})}{\varepsilon_{\mu}^2 + 1}, \quad (4)$$

where

$$\left(\frac{d^2\sigma}{dE_f d\Omega_f} \right)_{\text{dir}} = (2\pi)^4 m_p^2 \frac{K_f k_e}{K_i} \int |t_{\text{dir}}(E_i, \Omega_f, \mathbf{k}_e)|^2 d\Omega_e \quad (5)$$

is the DDCS of direct ionization. In the region of autoionization resonances, it forms a monotonic background. The other quantities are defined as

$$A_{\text{int},\mu}(\Omega_f, \varepsilon_{\mu}) = (2\pi)^4 m_p^2 \frac{K_f k_e}{K_i} 2 \operatorname{Re}\{t_{\text{exc},\mu}(\Omega_f)\} \int K_{\text{res},\mu}(\Omega_f, \mathbf{k}_e) t_{\text{dec},\mu}^0(\mathbf{k}_e) t_{\text{dir}}^*(\Omega_f, \mathbf{k}_e) d\Omega_e, \quad (6)$$

$$B_{\text{int},\mu}(\Omega_f, \varepsilon_{\mu}) = (2\pi)^4 m_p^2 \frac{K_f k_e}{K_i} 2 \operatorname{Im}\{t_{\text{exc},\mu}(\Omega_f)\} \int K_{\text{res},\mu}(\Omega_f, \mathbf{k}_e) t_{\text{dec},\mu}^0(\mathbf{k}_e) t_{\text{dir}}^*(\Omega_f, \mathbf{k}_e) d\Omega_e, \quad (7)$$

$$B_{\text{exc},\mu}(\Omega_f, \varepsilon_{\mu}) = (2\pi)^4 m_p^2 \frac{K_f}{K_i} |t_{\text{exc},\mu}(\Omega_f)|^2 k_e \int |K_{\text{res},\mu}(\Omega_f, \mathbf{k}_e)|^2 |t_{\text{dec},\mu}^0(\mathbf{k}_e)|^2 d\Omega_e. \quad (8)$$

It can be seen that $A_{\text{int},\mu}(\Omega_f, \varepsilon_\mu)$ and $B_{\text{int},\mu}(\Omega_f, \varepsilon_\mu)$ account for the interference of resonant and direct transitions, whereas $B_{\text{exc},\mu}(\Omega_f, \varepsilon_\mu)$ is proportional to the differential cross section of the excitation of LM -sublevels of the AIS

$$\frac{d\sigma_{\text{exc},\mu}}{d\Omega_f} = (2\pi)^4 m_p^2 \frac{K_f}{K_i} |t_{\text{exc},\mu}(\Omega_f)|^2. \quad (9)$$

In general, the quantities $A_{\text{int},\mu}(\Omega_f, \varepsilon_\mu)$, $B_{\text{int},\mu}(\Omega_f, \varepsilon_\mu)$ and $B_{\text{exc},\mu}(\Omega_f, \varepsilon_\mu)$ are a function of energy in the region of AI resonances since $K_{\text{res},\mu}(\Omega_f, \mathbf{k}_e)$ may rapidly vary in the vicinity of an autoionization resonance under the conditions of strong CIFS ($|\xi| \geq 1$). Therefore, they cannot be considered as resonance parameters and equation (4) as a parametric equation. Moreover, when the velocity of the scattered particle is close to the velocity of the ejected electron ($v_f \approx v_e$), there is a cusp in the direct ionization cross sections, and the interference terms $A_{\text{int},\mu}(\Omega_f, \varepsilon_\mu)$ and $B_{\text{int},\mu}(\Omega_f, \varepsilon_\mu)$ may manifest themselves in an additional dependence on the electron energy due to the rapid variation of the direct ionization amplitude. However, unlike resonances in electron emission spectra, integration over the emission angles of the ejected electron is likely to smoothen this latter effect out, while the electron energy dependence of $K_{\text{res},\mu}$ is of major importance at small ejection angles occupying a small portion of the total integration range. Therefore, one may expect that the resonance profiles in the energy loss spectra are closer to the classical Fano shape, unlike in angular distributions of ejected electrons, where significant distortions of AI resonances take place in the region of strong CIFS (Godunov *et al* 1997a).

Under weak or moderate CIFS, one can neglect the dependence of $K_{\text{res},\mu}$ on ε_μ and replace it with a constant $K_{\text{res},\mu}^0 = K_{\text{res},\mu}(\varepsilon_\mu = 0)$ (Godunov *et al* 1997a). Hence, equation (4) may be rewritten as a Shore-like (Shore 1967) parametrization of ionization cross sections:

$$\frac{d^2\sigma}{dE_f d\Omega_f} = \left(\frac{d^2\sigma}{dE_f d\Omega_f} \right)_{\text{dir}} + \sum_{\mu} \frac{A_{\mu}^0(\Omega_f)\varepsilon_{\mu} + B_{\mu}^0(\Omega_f)}{\varepsilon_{\mu}^2 + 1}, \quad (10)$$

with

$$A_{\mu}^0(\Omega_f) = (2\pi)^4 m_p^2 \frac{K_f k_e}{K_i} \int 2 \text{Re}\{K_{\text{res},\mu}^0 t_{\text{dec},\mu}^0 t_{\text{exc},\mu}^* t_{\text{dir}}^*\} d\Omega_e, \quad (11)$$

$$B_{\mu}^0(\Omega_f) = (2\pi)^4 m_p^2 \frac{K_f k_e}{K_i} \int (2 \text{Im}\{K_{\text{res},\mu}^0 t_{\text{dec},\mu}^0 t_{\text{exc},\mu}^* t_{\text{dir}}^*\} + |K_{\text{res},\mu}^0 t_{\text{dec},\mu}^0 t_{\text{exc},\mu}^*|^2) d\Omega_e. \quad (12)$$

It was noted (Godunov *et al* 1997a), however, that CIFS may still essentially modify the values of the profile parameters by $K_{\text{res},\mu}^0$, so that the resulting profile would be different from what one would get without the post-collision interaction.

2.2. Differential yield of an autoionization resonance

To extract important information on the mechanisms of autoionization from experiment using an efficient parametrization, high spectral resolution is required (Godunov *et al* 1997a, Moretto-Capelle *et al* 1997). In low-resolution experiments, or without an efficient parametrization of DDCS, one could use *differential yields* of resonances to estimate the dynamical characteristics of excitation and ionization. The differential yield is defined as the algebraic area under the resonance profile minus the direct ionization background:

$$\frac{dY_{\mu}}{d\Omega_f} = \int \frac{A_{\text{int},\mu}(\Omega_f, \varepsilon_{\mu}) \varepsilon_{\mu} + B_{\text{int},\mu}(\Omega_f, \varepsilon_{\mu}) + B_{\text{exc},\mu}(\Omega_f, \varepsilon_{\mu})}{\varepsilon_{\mu}^2 + 1} d(\Delta E). \quad (13)$$

Changing the integration variable to ε_{μ} with the use of energy conservation $E_i = E_f + E_e + I$, one obtains the differential yield of an autoionization resonance in the energy loss spectrum as

$$\frac{dY_{\mu}}{d\Omega_f} = K_{\text{exc},\mu} \frac{d\sigma_{\text{exc},\mu}}{d\Omega_f} + \frac{dY_{\text{int},\mu}}{d\Omega_f}, \quad (14)$$

with the coefficient in the excitation term being given by

$$K_{\text{exc},\mu} = \frac{\Gamma_\mu}{2} \int \frac{1}{\varepsilon_\mu^2 + 1} d\varepsilon_\mu \int |K_{\text{res},\mu}(\Omega_f, \mathbf{k}_e)|^2 |t_{\text{dec},\mu}^0(\mathbf{k}_e)|^2 k_e d\Omega_e, \quad (15)$$

and the interference term being explicated as

$$\frac{dY_{\text{int},\mu}}{d\Omega_f} = \frac{\Gamma_\mu}{2} \int \frac{A_{\text{int},\mu}(\Omega_f, \varepsilon_\mu) \varepsilon_\mu + B_{\text{int},\mu}(\Omega_f, \varepsilon_\mu)}{\varepsilon_\mu^2 + 1} d\varepsilon_\mu. \quad (16)$$

That is, the differential yield of an autoionization resonance includes two terms, one being proportional to the differential cross section of AIS excitation, and the other representing an interference contribution. We will consider a few important special cases of (14).

In the *eikonal approximation*, the coefficient $K_{\text{exc},\mu}$ in equation (14) equals 1. This can be demonstrated from the definition $K_{\text{exc},\mu}$ and the expressions for the CIFS factor $K_{\text{res},\mu}$ (3) and the AIS decay amplitude in an isolated atom, which can be written as (Godunov *et al* 1997b)

$$t_{\text{dec},\mu}^0 = \frac{\tau_{\text{dec},\mu}}{\sqrt{k_e} \Gamma_\mu / 2} \exp(i\sigma_L) Y_{LM}(\Omega_e), \quad (17)$$

where $\Gamma_\mu = 2\pi \tau_{\text{dec},\mu}^2$ and σ_L is the Coulomb phase of the wavefunction of a free electron in the field of a residual ion. Substituting these expressions into (15), we obtain

$$K_{\text{exc},\mu} = \int |Y_{LM}(\Omega_e)|^2 d\Omega_e \frac{\xi}{\sinh \pi \xi} \int \frac{\exp(-2\xi \arctan \varepsilon_\mu)}{\varepsilon_\mu^2 + 1} d\varepsilon_\mu = 1. \quad (18)$$

Hence, in the eikonal approximation, the differential yield contains an additive interference correction to the corresponding excitation cross section.

In the conditions of *moderate or weak CIFS* the Shore-like parametrization (10) becomes applicable, with the differential yield being proportional to parameter B_μ^0 :

$$\frac{dY_\mu}{d\Omega_f} = \frac{\pi \Gamma_\mu}{2} B_\mu^0(\Omega_f) = \frac{d\sigma_{\text{exc},\mu}}{d\Omega_f} + (2\pi)^4 m_p^2 \frac{K_f k_e}{K_i} \pi \Gamma_\mu \int \text{Im}\{K_{\text{res},\mu}^0 t_{\text{dec},\mu}^0 t_{\text{exc},\mu} t_{\text{dir}}^*\} d\Omega_e, \quad (19)$$

where we have used the definition (12) together with equation (18).

In the *first Born approximation*, when the influence of CIFS on the ionization amplitudes is negligible, one can derive an analytical expression for the interference term in (19). Setting $K_{\text{res},\mu}^0 = 1$ and expanding the Born amplitude of direct ionization in partial waves

$$t_{\text{dir}}^B = \frac{1}{\sqrt{k_e}} \sum_{lm} \exp(i\sigma_l) t_{\text{dir}}^{lm}(Q) Y_{lm}(\Omega_e), \quad (20)$$

integrating over ejection angles and using orthogonality for spherical functions with different lm (Messiah 1966)

$$\frac{dY_\mu}{d\Omega_f} = \frac{d\sigma_{\text{exc},\mu}}{d\Omega_f} + (2\pi)^4 m_p^2 \frac{K_f}{K_i} 2\pi \tau_{\text{dec},\mu} \text{Im}(t_{\text{exc},\mu} t_{\text{dir}}^{*LM}). \quad (21)$$

As follows from (21), there is only one partial amplitude of direct ionization that contributes to the interference term in the differential yield of the autoionization resonance, in the Born approximation (Balashov *et al* 1973), in contrast to electron spectra, where the interference term includes all the partial amplitudes of direct ionization.

In the *first Born approximation* in the projectile–atom interaction, direct ionization amplitudes $t_{\text{dir}}^{(lm)}$ are real, and the excitation amplitude can be written as (see equation (32) and definitions below) $t_{\text{exc},\mu}^{\text{B1}} = t_{\text{exc},\mu}^{\text{d1}} + t_{\text{exc},\mu}^{\text{c1}}$. Noting the relation of the *on-shell* part of

the amplitude of the inverse Auger process $t_{\text{exc},\mu}^{\text{cl,on}}$ to the Born amplitude of direct ionization (Godunov *et al* 1997b)

$$t_{\text{exc},\mu}^{\text{cl,on}} = -i\pi \tau_{\text{dec},\mu} t_{\text{dir}}^{LM}, \quad (22)$$

and neglecting the *off-shell* part of the inverse Auger amplitude, we transform equation (21) into

$$\frac{dY_\mu}{d\Omega_f} = \frac{d\sigma_{\text{exc},\mu}}{d\Omega_f} - \pi \Gamma_\mu \frac{d\sigma_{\text{dir}}^L}{d\Omega_f}. \quad (23)$$

This expression is a special case of the general result obtained in Godunov *et al* (1997c), and it allows one to treat the differential yield as a lower estimate for autoionization cross sections at high energies.

2.3. Computational model

We have calculated the profiles and differential yields of autoionization resonances in the energy loss spectra of protons scattered from atomic helium. Two basic forms of ionization amplitude (2) were used.

CIFS amplitudes:

$$t_{\text{fi}} = t_{\text{dir}} + \sum_{\mu} \frac{K_{\text{res},\mu}(\varepsilon_\mu) t_{\text{dec},\mu}^0 t_{\text{exc},\mu}}{\varepsilon_\mu + i}. \quad (24)$$

The amplitude of direct ionization allowing for CIFS and which is applicable for all scattering angles has been obtained in Godunov *et al* (1998):

$$\begin{aligned} t_{\text{dir}} = & K_{\text{dir}} t_{\text{dir}}^B(\mathbf{Q}) - \frac{2M_{\text{pt}} Z_p^2 f_c^{(+)}(v_{12}) f_c^{(+)}(v_{13})}{\pi^2 v_f} (1 + d_{12})^{i v_{12}} \\ & \times \int \frac{T_{\text{fi}}(0, \mathbf{Q} - \mathbf{p}) - T_{\text{fi}}(0, \mathbf{Q})}{p^2 |\mathbf{Q} - \mathbf{p}|^2 (p_z - i0)} d\mathbf{p} \\ & - \frac{2M_{\text{pt}} Z_p^2 f_c^{(+)}(v_{12}) f_c^{(+)}(v_{13})}{\pi^2 v_f} (1 + d_{13})^{i v_{13}} \int \frac{Z_t(0, \mathbf{p}) - T_{\text{fi}}(\mathbf{Q} - \mathbf{p}, \mathbf{p})}{p^2 |\mathbf{Q} - \mathbf{p}|^2 (p_z - i0)} d\mathbf{p}, \end{aligned} \quad (25)$$

where $d_{ij} = 2k_{ij}Q/Q^2$, $\mathbf{Q} = \mathbf{K}_i - \mathbf{K}_f$ is the projectile momentum transfer to the target, M_{pt} is the reduced mass of the target + projectile, Z_p and Z_t are the projectile and target nucleus charge respectively and

$$K_{\text{dir}} = f_c^{(+)}(v_{12}) f_c^{(+)}(v_{13}) (1 + d_{12})^{i v_{12}} (1 + d_{13})^{i v_{13}} {}_2F_1(-i v_{12}, -i v_{13}, 1, X), \quad (26)$$

with

$$X = 2 \frac{2(k_{12}Q)(k_{13}Q) - Q^2(k_{12}k_{13} - k_{12}k_{13})}{(Q^2 + 2k_{12}Q)(Q^2 + 2k_{13}Q)}. \quad (27)$$

The quantity T_{fi} , given by

$$T_{\text{fi}}(\mathbf{s}, \mathbf{p}) = \frac{1}{\sqrt{2}} \int \int \phi_f^*(\mathbf{r}'_{23}) \phi_{k_{23}}^{(-)*}(\mathbf{r}_{23}) \exp(i\mathbf{s}\mathbf{r}'_{23} + i\mathbf{p}\mathbf{r}_{23}) \phi_i(\mathbf{r}'_{23}, \mathbf{r}_{23}) d\mathbf{r}'_{23} d\mathbf{r}_{23}, \quad (28)$$

is the two-particle matrix element for the transition from the ground state of atomic helium represented by the wavefunction ϕ_i to the final state described by the wavefunction ϕ_f of the residual ion He^+ and the continuous-spectrum wavefunction of the ejected electron moving in the field of the residual ion $\phi_{k_{23}}^{(-)}$. We note that the first term in the amplitude (25), commonly

known as *peaking* amplitude, does not contain any projectile–target nucleus interaction in the transition operator and is only applicable for angles $\theta_f \leq 1/M_p$ mrad (Godunov *et al* 1998).

Born amplitudes:

$$t_{fi}^B = t_{dir}^B + \sum_{\mu} \frac{t_{dec,\mu}^{\circ} t_{exc,\mu}}{\varepsilon_{\mu} + i}. \quad (29)$$

In the Born amplitude of direct ionization, we accounted for the first two terms in the projectile–target interaction:

$$t_{dir}^B = t_{dir}^{B1} + t_{dir}^{B2}. \quad (30)$$

The ground state of the target has been included in the intermediate state set in the amplitude t_{dir}^{B2} . Since the contribution of all the other intermediate states is small, t_{dir}^{B2} could be calculated as

$$t_{dir}^{B2} = \frac{Z_p}{\pi^2 v_f} \int \frac{T_{fi}(0, \mathbf{Q} - \mathbf{p}) t_{ii}^{B1}(\mathbf{p})}{|\mathbf{Q} - \mathbf{p}|^2 (p_z + i0)} d\mathbf{p}, \quad (31)$$

where t_{ii}^{B1} is the amplitude of elastic scattering of proton on helium in the first Born approximation, containing the projectile–core interaction in the transition operator.

Correlated wavefunctions were determined by the MCHF method (Froese-Fischer 1977), the wavefunction for a free electron was calculated in the frozen-core Hartree–Fock approximation (Cowan 1981). For $t_{exc,\mu}^{d2}$, the singlet states of one-electron excitation $|1snl\rangle$ with $n = 2, 3$ were included in the intermediate state set.

The AIS excitation amplitude can be expanded in powers of the projectile’s interaction with the target, and we consider the first Born (1) and second Born (2) terms in this work. Also, since the AIS are not plain discrete states, there are contributions from the transitions to both its bound (d) and continuous components (c) in the full excitation amplitude $t_{exc,\mu}$ (Godunov *et al* 2000); for the present discussion, we use an approximate expression for $t_{exc,\mu}$:

$$t_{exc,\mu} = t_{exc,\mu}^{d1} + t_{exc,\mu}^{c1} + t_{exc,\mu}^{d2} + t_{exc,\mu}^{c2}. \quad (32)$$

The first term, commonly referred to as ‘shake up’, describes direct two-electron excitation of the discrete-spectrum component of the AIS, which is essentially due to electron correlation in the target. The second term $t_{exc,\mu}^{c1}$, also known as ‘TS-1’, includes target ionization in a single interaction linked to the bound component of the AIS by electron correlation; in particular, this term describes an inverse Auger process following the ionization of a single electron (Schulz *et al* 1995). The third term describes various kinds of cascade excitation due to successive interactions with the projectile (‘TS-2’ term); in this work, it is only excitation through the intermediate states of one-electron excitation that has been considered. The c1 and d2 amplitudes strongly interfere with each other (Godunov *et al* 2000). The sum $t_{exc,\mu}^{c1} + t_{exc,\mu}^{d2}$ could be called the generalized amplitude of two-step excitation. The last $t_{exc,\mu}^{c2}$ term accounts for the second-order transitions to the continuum linked to the AIS through electron correlations.

3. Results

We have calculated the profiles and differential yields for the lowest autoionization resonances $(2s^2) \ ^1S$, $(2p^2) \ ^1D$ and $(2s2p) \ ^1P$ of helium colliding with 100 and 150 keV protons. Differential yields are compared with experimental data of Schulz *et al* (1995).

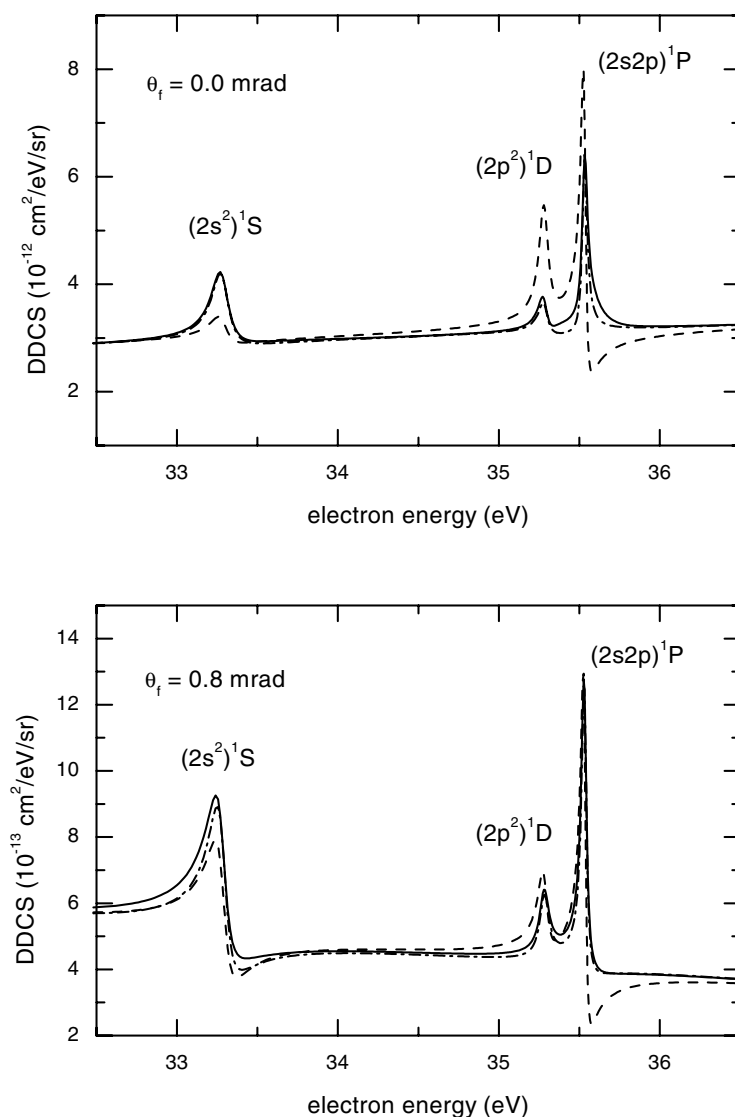


Figure 1. Theoretical profiles of the autoionization resonances $(2s^2)^1S$, $(2p^2)^1D$ and $(2s2p)^1P$ of helium excited by 100 keV proton impact in the energy loss spectra of scattered protons. Scattering angles are 0.0 and 0.8 mrad. —: full calculation with CIFS and projectile–core interaction, equations (4 and 24); ---: calculation in the second Born approximation without CIFS influence; — · —: calculation with CIFS but assuming Fano shape for resonance profiles, equation (10).

3.1. Resonance profiles

Theoretical profiles of autoionization resonances in energy loss spectra calculated for proton energy of 100 keV and scattering angles of 0.0 and 0.8 mrad are presented in figure 1. To illustrate the importance of the CIFS in the resonance profiles, both CIFS and Born calculations are displayed. Since the influence of CIFS on direct ionization we discussed before (Godunov *et al* 1998), and for better comparison of resonance shapes, the calculations in different approximations were superimposed on the same experimental direct ionization background at the point corresponding to 29 eV (Schulz *et al* 1996). As one can see, CIFS distortions

are mainly quantitative in the case considered. In contrast to ejected electron spectra, there are no such CIFS effects as asymmetrical broadening or resonance splitting. The character of distortion is not influenced much by the collision kinematics, in contrast to abrupt changes in the resonance shapes with increasing ejection angle observed in electron spectra.

To explore the applicability of the Shore parametrization, we have also drawn in figure 1 the results of the complete CIFS calculation (with energy-dependent A_μ and B_μ defined by (4)) together with the Fano curve with constant parameters A_μ^0 and B_μ^0 defined by (10). As one can observe, the constant-parameter approximation works well enough, leading to errors much smaller than those associated with neglecting CIFS. Thus, at 100 keV proton collision energy and above, one can use Shore parametrization modified for energy loss spectra (10).

The proximity of the $(2p^2)^1D$ resonance to the strong $(2s2p)^1P$ resonance may mask the former in a low-resolution experiment. We have carried out calculations of the theoretical profiles of autoionization resonances of helium both without accounting for experimental resolution and convoluted with an apparatus Gaussian function with varying dispersion. At high resolution (0.1 eV), as expected, the shape of resonances does not change much. At a resolution of 0.5 eV, the $(2p^2)^1D$ and $(2s2p)^1P$ resonances are already merged. The point at the maximum of the peak corresponding to the combination of $(2p^2)^1D + (2s2p)^1P$ is differently predicted by the Born and CIFS calculations. At a poorer resolution of 1.5 eV, that corresponds to the resolution in the experiment (Schulz *et al* 1995), the two resonances look like one very broad peak. Moreover, all the most important details of the resonance shape are obscured at this energy resolution. Therefore, the resonance yield became the quantity of primary attention in this paper.

3.2. Differential yields of the autoionization resonances

The differential yield of an autoionization resonance is a quantity characterizing the overall contribution of the resonance to the ionization cross section. Yields are suitably defined in terms of a Shore-like parametrization (10), so that the differential yield is proportional to the parameter B_μ^0 . However, with a strong CIFS, such a parametrization becomes unphysical, and one has to calculate yields by numerical integration. This leads to additional error sources in processing experimental spectra, essentially depending on the background subtracting procedure, finite resolution and the choice of integration limits. Nevertheless, with all the reservations one can use differential yields to obtain an insight into the mechanisms of autoionization resonance formation in energy loss spectra.

Differential yields of autoionization resonances in the spectra of scattered protons are shown in figures 2–5, both calculated in various approximations and experimentally obtained by Schulz *et al* (1995). We present the sum of the $(2s2p)^1P$ and $(2p^2)^1D$ yields only, since the two resonances have not been resolved in the experiment. For comparison, we also display calculated excitation cross sections, which coincide with the excitation term of the yield in the eikonal approximation. Thus we can estimate the importance of the interference of resonant and direct transitions in the yields.

For both the CIFS and the Born calculation, the differential yield of autoionization resonances is a monotonically decreasing function of the scattering angle; the same holds for the corresponding excitation cross section. The absolute value of the yield depends both on the mechanisms of AIS excitation and the magnitude of its interference component, which appears to be sensitive to the accuracy of describing projectile–target interactions, such as CIFS and second-order processes. The scale and character of the influence of these mechanisms on the differential yield varies from one resonance to another, being more dependent on the scattering angle than on the proton energy. That is why we have chosen to consider angular dependencies of differential yields for each resonance at a fixed collision energy.

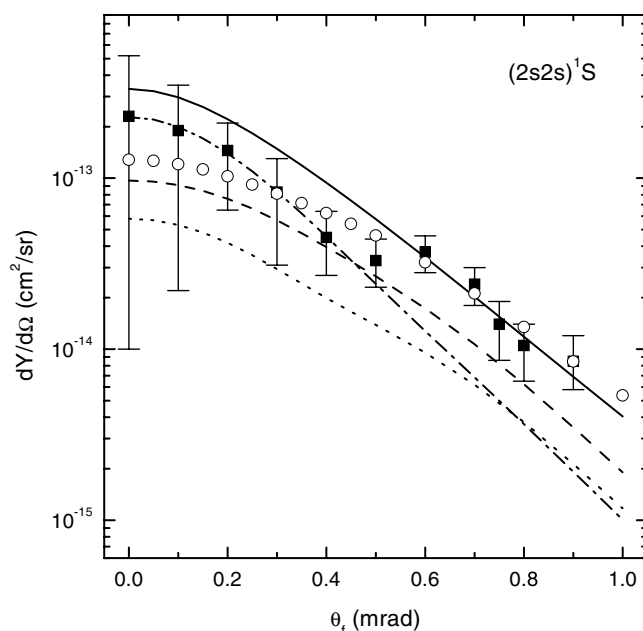


Figure 2. The differential yield of the $(2s^2)^1S$ autoionization resonance of helium in the energy loss spectra of 100 keV protons. —: calculation with CIFS and projectile–core interaction; - - -: calculation with CIFS, but without projectile–core interaction; ·····: calculation in the first Born approximation; - · - ·: calculation in the second Born approximation; ■: experimental data of Schulz *et al* (1995); ○: theoretical differential cross section $d\sigma_{\text{exc}}/d\Omega_f$ for double electron excitation.

The results of the full calculation for the $(2s^2)^1S$ resonance (figure 2) are in reasonable agreement with the experimental data. It can be seen that the calculations without either CIFS or projectile–core interaction are well below the full calculation. The first Born approximation strongly underestimates the differential yield for this collision energy for all scattering angles. One could also note a bump in the experimental differential yield between 0.04 and 0.08 mrad at 100 keV proton impact. Our calculations do not reproduce this structure showing a smooth dependence on the scattering angle. The semiclassical coupled channel calculations of Martin and Salin (1995) did not display such experimental behaviour. Thus, the question for this bump remains open.

For the sum of the $(2p^2)^1D$ and $(2s2p)^1P$ resonances (figures 3 and 5), the experimental points alternate around the theoretical curve for the total differential yield, which practically coincides with the sum of the corresponding excitation cross sections. In our calculations, the contribution from the $(2s2p)^1P$ resonance dominates in the sum (see figure 6), determining its qualitative behaviour. However, a more accurate model of the excitation of the $(2p^2)^1D$ resonance might change this result, since our calculations underestimate total excitation cross sections for this resonance in the energy region considered (Moretto-Capelle *et al* 1997). In semiclassical coupled channel equations without inclusion of the CIFS the 1D resonance yield dominates over the 1P yield at small scattering angle, whereas the opposite is observed for larger values of the scattering angles θ_f .

The difference between the differential yield and the excitation cross section (and hence the role of the Fano interference of resonance excitation with direct ionization) could be investigated in more detail considering the relative deviation of $d\sigma_{\text{exc},\mu}/d\Omega_f$ from $dY_\mu/d\Omega_f$

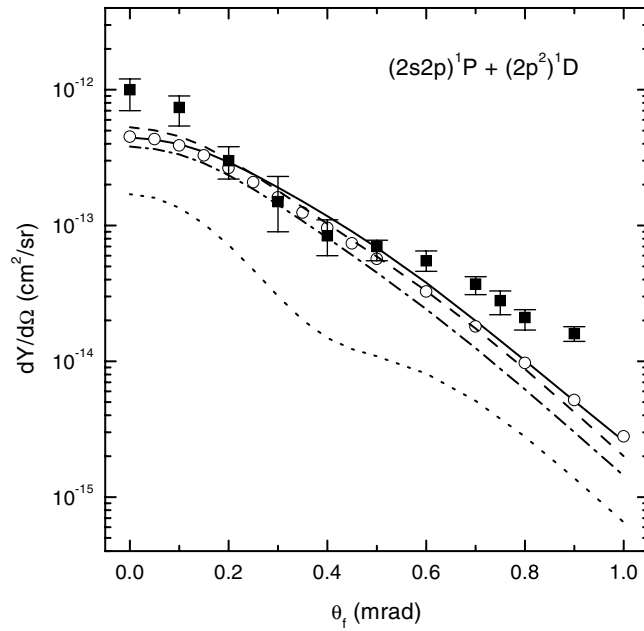


Figure 3. Differential yield of the sum of the $(2p^2)^1D$ and $(2s2p)^1P$ autoionization resonances of helium in the energy loss spectra of 100 keV protons. Notation as in figure 2.

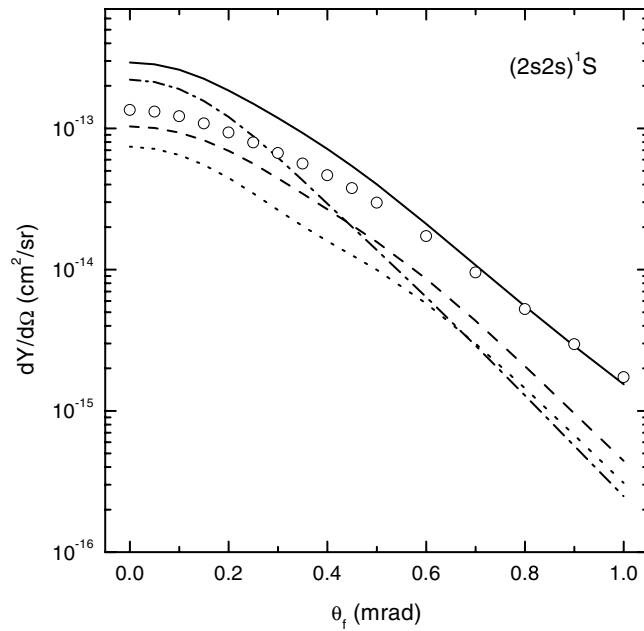


Figure 4. Differential yield of the $(2s^2)^1S$ autoionization resonance of helium in the energy loss spectra of 150 keV protons. Notation as in figure 2.

presented in figures 2–5. It should be noted that the interference terms $dY_{\text{int},\mu/d}\Omega_f$ are essential to properly describe the resonant yield of the $(2s^2)^1S$ resonance at small scattering angles, where one cannot use differential yields to evaluate AIS excitation. This result is in accordance

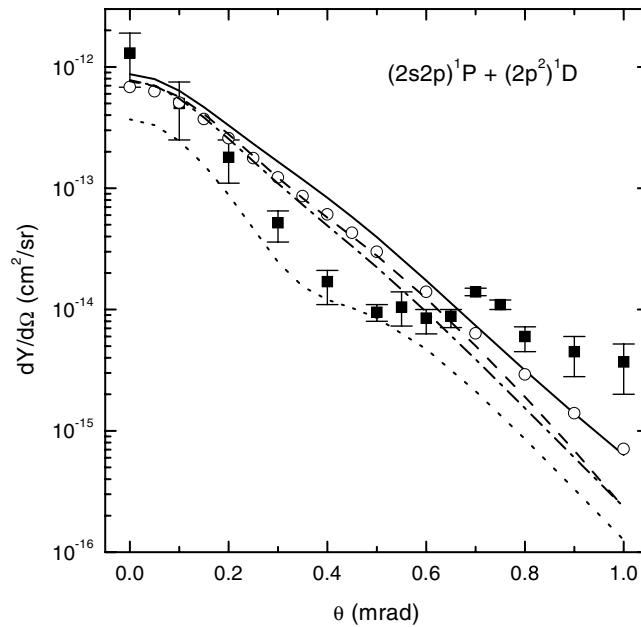


Figure 5. Differential yield of the sum of the $(2p^2)^1D$ and $(2s2p)^1P$ autoionization resonances of helium in the energy loss spectra of 150 keV protons. Notation as in figure 2.

with our analysis for the *total resonance* yield and excitation cross section (Godunov *et al* 1997c, figure 2). It was demonstrated that the resonance yield can provide a lower estimate for excitation cross section but for asymptotic collision velocities. At intermediate collision energies there may be points where the resonance yield is equal to excitation cross section but it cannot be considered as a typical phenomenon. However, from figures 2–5 it can be seen that for scattering angles large then 0.6 mrad the resonance yield and double excitation cross section practically come together.

3.3. Mechanisms of excitation and yield formation

In equation (32), we have written the total amplitude of AIS excitation as a sum of four components representing different excitation mechanisms. To explore the interplay of these contributions, we have calculated AIS excitation cross sections for the three lowest AIS of helium excited by proton impact, differential in the projectile scattering angle, for a number of projectile energies. The results are displayed for a projectile energy of 100 keV in figure 6.

Figure 6 illustrates the relative significance of the d1, d2 and c1 channels in AIS excitation by 100 keV protons—the qualitative picture remains the same for other proton energies. Here, we did not present the c2 mechanism. We found numerically that generally the $t_{exc,\mu}^{c2}$ term in the excitation amplitude is small. As one can see, the d1 contribution dominates at small scattering angles for the $(2s^2)^1S$ and $(2s2p)^1P$ resonances, despite the fact that the contribution of each of the amplitudes $t_{exc,\mu}^{c1}$ and $t_{exc,\mu}^{d2}$ is significant—however, their destructive interference makes their combined contribution small enough at small scattering angles. The presence of such a strong interference has been demonstrated earlier in electron spectra (Godunov *et al* 1997a), and it has been suggested that the sum of the $t_{exc,\mu}^{c1}$ and $t_{exc,\mu}^{d2}$ amplitudes be called the generalized amplitude of two-step excitation. These two-step mechanisms seems to be more important

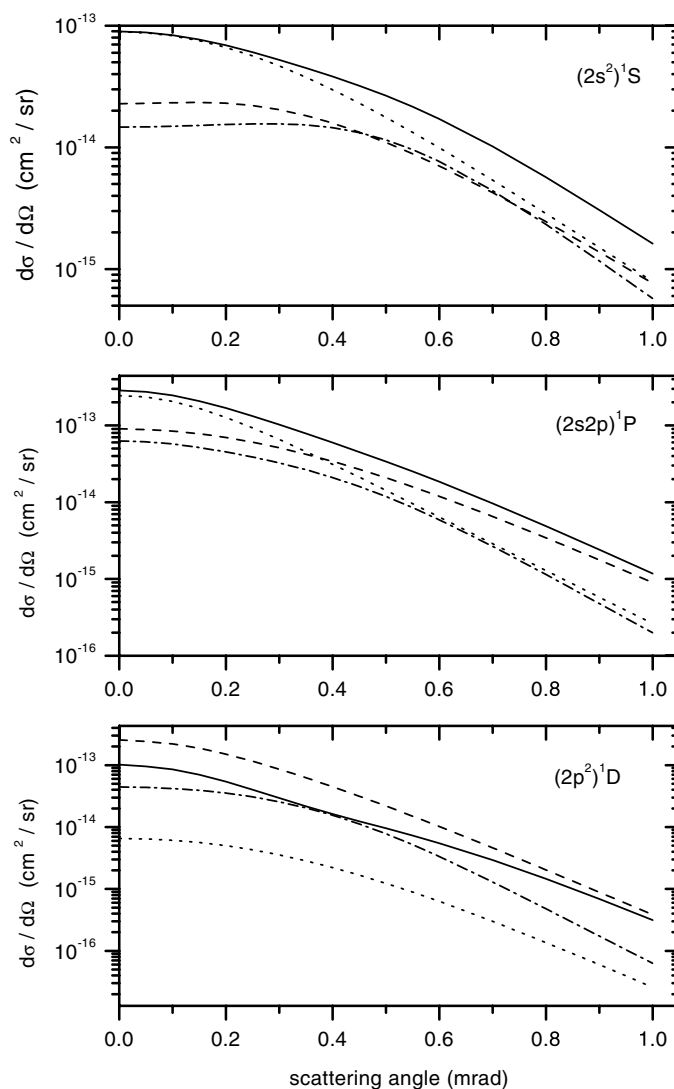


Figure 6. The differential excitation cross section for the $(2s^2)^1S$, $(2s2p)^1P$ and $(2p^2)^1D$ resonances in helium excited by 100 keV protons; solid line—calculation with excitation amplitude $f_{\text{exc}} = f_{d1} + f_{d2} + f_{c1}$; \cdots : contribution of the d1-mechanism ($f_{\text{exc}} = f_{d1}$); $---$: contribution of the d2-mechanism ($f_{\text{exc}} = f_{d2}$); $- \cdot -$: contribution of the c1-mechanism ($f_{\text{exc}} = f_{c1}$).

for the $(2p^2)^1D$ resonance, where it significantly contributes to the total excitation cross section. However, we cannot be sure enough, since there are indications that the excitation amplitude is underestimated for this resonance in our present calculations (Godunov *et al* 2000). Pronounced interference effects require that interfering amplitudes are of comparable magnitudes. Therefore, a more realistic description of the d2 amplitudes (or allowing for third order terms) for the $(2p^2)^1D$ resonance might lead to a pronounced interference pattern, which is currently only indicated at about 0.7 mrad. This could explain the peak structure seen in the experimental data that is not reproduced by the current calculations.

Extracting information on the mechanisms of AIS excitation is an important part of comparative analysis of the scattering spectra with the spectra of ejected electrons, which

are complementary in that energy distributions of ejected electrons at a fixed ejection angle contain *total* excitation cross sections, while energy distributions of protons at a fixed scattering angle contain *differential* cross sections. Therefore, the sets of electron and proton spectra taken together give complete information on AIS excitation. The peculiarities of the CIFS influence and the interference of direct and resonant ionization in scattering spectra favour an investigation of differential excitation cross sections. As follows from our calculations, differential yields of autoionization resonances can be used as estimates for excitation cross sections, and a consistent accounts for both CIFS and projectile–core interaction generally improves the accuracy of such an approximation.

4. Conclusions

The shape of both theoretical and experimental profiles of autoionization resonances in energy loss spectra is weakly dependent on the collision kinematics (scattering angle and proton energy), varying rather smoothly. The distortion of resonance profiles due to CIFS is mainly quantitative. This is different from the behaviour of ejected electron spectra. Shore parametrization for energy loss spectra (equation (10)) can be applied for processing of experimental resonance profiles for collision energy of 100 keV and above. Simultaneous accounts for CIFS and higher-order projectile–core interactions may suppress the interference component in the differential yield of the resonance, making it closer to the corresponding AIS excitation cross section. For scattering angles larger than 0.6 mrad the interference component is small. This makes it possible to use differential yields to estimate AIS excitation cross sections differential in the scattering angle, which provides additional information, as compared to that obtained from electron spectra.

Acknowledgments

AG acknowledges support from the Division of Chemical Sciences, Office of Basic Energy Sciences, Office of Energy Research, US Department of Energy. MS acknowledges support from the National Science Foundation.

References

- Arcuni P W and Schneider D 1987 *Phys. Rev. A* **36** 3059–70
Balashov V V, Lipovetskii S S and Senashenko V S 1973 *Sov. Phys.–JETP* **36** 858–60
Bordenave-Montesquieu A, Moretto-Capelle P, Gleizes A, Andriamonje S, Martin F and Salin A 1995 *J. Phys. B: At. Mol. Opt. Phys.* **28** 653–70
Cowan R D 1981 *The Theory of Atomic Structure and Spectra* (Los Angeles: University of California Press)
Fano U 1961 *Phys. Rev.* **124** 1866–78
Froese-Fischer C 1977 *The Hartree–Fock Method for Atoms* (New York: Wiley)
Godunov A L, Kunikeev Sh D, Novikov N V and Senashenko V S 1989 *Sov. Phys.–JETP* **69** 927–33
Godunov A L, Schipakov V A, Moretto-Capelle P, Bordenave-Montesquieu D, Benhenni M and Bordenave-Montesquieu A 1997a *J. Phys. B: At. Mol. Opt. Phys.* **30** 5451–77
Godunov A L, McGuire J H and Schipakov V A 1997b *J. Phys. B: At. Mol. Opt. Phys.* **30** 3227–45
Godunov A L, Ivanov P B and Schipakov V A 1997c *J. Phys. B: At. Mol. Opt. Phys.* **30** 3403–15
Godunov A L, Ivanov P B, Schipakov V A, Moretto-Capelle P, Bordenave-Montesquieu D and Bordenave-Montesquieu A 2000 *J. Phys. B: At. Mol. Opt. Phys.* **33** 971–99
Godunov A L, Schipakov V A and Schulz M 1998 *J. Phys. B: At. Mol. Opt. Phys.* **31** 4943–60
Htwe W, Vajnai T, Barnhart M, Gauss A D and Schulz M 1994 *Phys. Rev. Lett.* **73** 1348–51
Kamber E Y, Cocke C L, Cheng S and Varghese S L 1988a *Phys. Rev. Lett.* **60** 2026–9
Kamber E Y, Cocke C L, Cheng S, McGuire J H and Varghese S L 1988b *J. Phys. B: At. Mol. Opt. Phys.* **21** L455–9

- Kvale T J, Seely D G, Blankenship D M and Park J T 1985 *Phys. Rev. A* **32** 1369–78
- Martin F and Salin A 1995 *J. Phys. B: At. Mol. Opt. Phys.* **28** 1985–94
- Messiah A M 1996 *Quantum mechanics* (New York: Wiley)
- Moretto-Capelle P, Benhenni M, Bordenave-Montesquieu D and Bordenave-Montesquieu A 1996 *J. Phys. B: At. Mol. Opt. Phys.* **29** 2007–20
- Moretto-Capelle P, Bordenave-Montesquieu D, Bordenave-Montesquieu A, Godunov A L and Schipakov V A 1997 *Phys. Rev. Lett.* **79** 5230–3
- Pedersen J O P and Hvelplund P 1989 *Phys. Rev. Lett.* **62** 2373–6
- Rodriguez V D and Barrachina 1998 *Phys. Rev. A* **57** 215
- Rudd M E, Kim Y K, Madison D H and Gay T J 1992 *Rev. Mod. Phys.* **64** 441
- Schulz M 1995 *Int. J. Mod. Phys. B* **9** 3269–301
- Schulz M, Htwe W T, Gauss A D, Peacher J L and Vajnai T 1995 *Phys. Rev. A* **51** 2140–50
- Schulz M, Vajnai T, Gaus A D, Htwe W, Madison D H and Olson R E 1996 *Phys. Rev. A* **54** 2951–61
- Shore B W 1967 *J. Opt. Soc. Am.* **57** 881–7
- Stolterfoht N 1987 *Phys. Rep.* **146** 315–424
- Ullrich J *et al* 1994 *Comments At. Mol. Phys.* **30** 285–94 and references therein